



HAL
open science

What Quantum Chemical Simulations tell us about the Infrared Spectra Structure and Interionic Interactions of a Bulk Ionic Liquid

Sergey Katsyuba, Elena Zvereva

► **To cite this version:**

Sergey Katsyuba, Elena Zvereva. What Quantum Chemical Simulations tell us about the Infrared Spectra Structure and Interionic Interactions of a Bulk Ionic Liquid. *Physical Chemistry Chemical Physics*, 2022, 24 (12), pp.7349 - 7355. 10.1039/d1cp05745f . hal-03655002

HAL Id: hal-03655002

<https://ifp.hal.science/hal-03655002>

Submitted on 29 Apr 2022

HAL is a multi-disciplinary open access archive for the deposit and dissemination of scientific research documents, whether they are published or not. The documents may come from teaching and research institutions in France or abroad, or from public or private research centers.

L'archive ouverte pluridisciplinaire **HAL**, est destinée au dépôt et à la diffusion de documents scientifiques de niveau recherche, publiés ou non, émanant des établissements d'enseignement et de recherche français ou étrangers, des laboratoires publics ou privés.

What quantum chemical simulations tell us about the infrared spectra, structure and interionic interactions of a bulk ionic liquid

Sergey A. Katsyuba*^a and Elena E. Zvereva*^{ab}

The recently developed efficient protocol to explicit quantum mechanical modeling of the structure and IR spectra of liquids and solutions [Katsyuba *et al.*, *J. Phys. Chem. B*, 2020, **124**, 6664–6670] is applied to ionic liquid 1-ethyl-3-methyl-imidazolium tetrafluoroborate [Emim][BF₄], and its C2-deuterated analog [Emim-d][BF₄]. It is shown that the solvation strongly modifies the frequencies and IR intensities of both cationic and anionic components of the ionic liquids. The main features of the bulk spectra are reproduced by the simulations for cluster ([Emim][BF₄])₈, representing an ion pair solvated by the first solvation shell. The geometry of the cluster closely resembles the solid-state structure of the actual ionic liquid and is characterized by short contacts of all CH moieties of the imidazolium ring with [BF₄][−] anions. Both structural and spectroscopic analyses allow the contacts to be interpreted as hydrogen bonds of approximately equal strength. The enthalpies of these liquid-state H-bonds, estimated with the use of empirical correlations, amount to 1.2–1.5 kcal mol^{−1}, while the analogous estimates obtained for the gas-phase charged species [Emim][BF₄]₂[−] and [Emim]₂[BF₄]⁺ increase to 3.6–3.9 kcal mol^{−1}.

1. Introduction

Ionic liquids (ILs), organic salts with low melting points, have reached practically all areas of science and industry. Their useful properties, and possibilities for their tuning on the basis of near limitless available combinations of ionic components of ILs, is the main reason for this wide spread.¹ At the same time, the sheer number of possible variations of both cations and anions constituting ILs requires structure–property relationships for tailoring their properties. A thorough understanding of how the properties of an IL arise from its structure is impossible without knowledge of the supramolecular architecture of the IL and the forces acting between its elements. Infrared (IR) spectroscopy is one of the most popular experimental methods used to establish the abovementioned features.² To derive structural information from IR spectra, input is required from quantum chemical calculations at computational levels that match the experimental resolution and accuracy. The latter condition is achievable in most cases of gas-phase studies, but it is very problematic for the condensed state.³ In particular, IR spectra of

bulk ILs differ dramatically from the spectra of their isolated cationic and/or anionic components.⁴

Molecular dynamics (MD) simulations of both molecular^{5,6} and ionic liquids,⁷ allow the liquid-state IR spectra to be obtained *via* Fourier transform of the velocity autocorrelation function in the MD trajectory. However, the most rigorous *ab initio* MD^{6,7} approach involves a huge amount of computer resources while the accuracy of the theoretical spectra obtained on the grounds of classical molecular mechanical treatment of the liquid strongly depends on the quality of the applied empirical force fields.⁸ Recently, we presented an efficient approach to an accurate, fully quantum-mechanical (QM) modeling of IR spectra of condensed-phase systems.⁹ An automated cluster generation algorithm was applied to construct an ensemble of explicitly solvated molecular clusters that were re-optimized at a reasonable but efficient level of Density Functional Theory (DFT). The DFT simulated IR spectrum of the system matches the corresponding condensed-phase IR experiment better than the theoretical spectrum of the isolated molecule compared to the gas-phase IR spectrum. More details can be found in Section 2.

Our approach was successfully tested on hydrogen-bonded molecular liquids, such as methanol⁹ and ethanol,¹⁰ and aqueous and methanolic solutions of methyl lactate.⁸ It has been suggested that vibrational modes and dipole moment derivatives are mainly influenced by their immediate local surroundings, and the inclusion of the first solvation shell is sufficient to simulate liquid-phase IR spectra with similar

^a Arbuzov Institute of Organic and Physical Chemistry, FRC Kazan Scientific Centre of RAS, Arbuzov st. 8, 420088, Kazan, Russia. E-mail: skatsyuba@yahoo.com

^b IFP Energies Nouvelles, 1 et 4 avenue de Bois-Préau, 92852 Rueil-Malmaison Cedex, France

Electronic supplementary information (ESI) available: Optimized geometries and simulated IR spectra of various clusters. See DOI: 10.1039/d1cp05745f

accuracy as for individual molecules in a vacuum. In this work, we apply this protocol to prototypic room-temperature IL 1-ethyl-3-methyl-imidazolium tetrafluoroborate $[\text{Emim}][\text{BF}_4]$, where apart from hydrogen bonds (HBs), long-range Coulomb interactions are present. The purpose of our study is two-fold: (i) to improve our understanding of the factors influencing the IR spectra of condensed-phase systems in general, and (ii) to gain new knowledge about how these factors are reflected in the IR spectra of ILs, to search for spectroscopic markers of various structural subunits in the bulk IL, and to assess the strength of HBs functioning therein.

2. Computations

The IL was approximated by a representative ensemble of molecular clusters. In these clusters, solvation shells around the “solute” are formed by interaction with explicit “solvent” molecules. Both the “solute” and “solvent” species were represented by ion pairs consisting of cation $[\text{Emim}]^+$ and anion $[\text{BF}_4]^-$ (Fig. 1). Clusters were generated by the Quantum Cluster Growth (QCG) algorithm¹¹ which, in short, adds solvent molecules around the solute at energetically favorable positions using an intermolecular force field docking algorithm (xTB-IFF).¹² The cluster generation step is followed by MD simulations in which equilibrated snapshots from the trajectory are fully geometry optimized at the robust and fast semi-empirical GFN2-xTB¹³ level, forming an ensemble of low-energy clusters. To simulate the liquid $[\text{Emim}][\text{BF}_4]$ clusters, 4 to 8 ion pairs were taken into account. The cluster of lowest free energy (*i.e.*, including thermostistical corrections) was used as the starting point for the calculation of the IR spectra of the liquid. It should be noted that a comparison of the IR spectra calculated for clusters that are populated by more than 20% has shown that the difference between the spectrum of the lowest-energy cluster and all other clusters from the final ensemble is practically negligible (Fig. S1, ESI[†]).

For a more accurate treatment of explicit solvent effects, the GFN2-xTB generated clusters were re-optimized with the B97-3c composite DFT method,¹⁴ and harmonic vibrational frequencies

and IR intensities were calculated analytically. This highly efficient method has been shown¹⁵ to perform well for IR spectra computations in the harmonic approximation, being only slightly inferior to B3LYP – one of the best performing DFT methods for the calculation of vibrational frequencies and IR intensities of organic molecules.^{3,16} For better agreement with the experimental anharmonic frequencies, the computed harmonic frequencies with $\nu > 1100 \text{ cm}^{-1}$ were scaled by 0.979.¹⁰

The collective vibrations of clusters $([\text{Emim}][\text{BF}_4])_n$ involve species at the external surface of a cluster, which have no analogs in the case of the bulk IL. In order to minimize these finite cluster size effects, we separated the vibrations of the central ion pair $[\text{Emim}][\text{BF}_4]$ from the vibrations of the surrounding ions by increasing the atomic masses of the latter species to 400 amu, and thus shifting their vibrations to the low-frequency region (these separated spectra are represented in Fig. 3 and Tables 2–4). For comparison with experimental spectra, the computed absolute intensities (km mol^{-1}) were plotted against computed frequencies, with a Lorentzian broadening ($\text{fwhm} = 15 \text{ cm}^{-1}$). All DFT calculations were carried out using the Turbomole-7.5.1 program package.¹⁷

3. Results and discussion

3.1. Structure of $([\text{Emim}][\text{BF}_4])_n$ clusters.

The $[\text{Emim}]^+$ cation can adopt not only the nonplanar conformation shown in Fig. 1A, but also a planar form with the ethyl moiety eclipsing the C2–H bond. The nonplanar conformer, which is known to dominate both in the isolated cation and in the liquid $[\text{Emim}][\text{BF}_4]$,¹⁸ was used as the starting structure of the ion pair (Fig. 1A) for the generation of clusters $([\text{Emim}][\text{BF}_4])_n$. No conversion from the nonplanar to the planar conformer was obtained during the process of the cluster growth (see Section 2), and thus, the relative abundance of the $[\text{Emim}]^+$ conformers within the clusters did not coincide with the real IL, where the planar cations were still detected by Raman spectroscopy.¹⁸ Nevertheless, this structural deviation of our models from the experiment is of minor importance for the cluster simulations of IR spectra, since the mid-IR spectrum of the IL is practically insensitive to the cation conformation.^{19,20}

Variation of the number (n) of ion pairs in the clusters $([\text{Emim}][\text{BF}_4])_n$ demonstrates that formation of the first solvation shell of the $[\text{Emim}]^+$ cation is accomplished at $n = 8$ (Fig. 1A). The protons of the solvated cation in this cluster form short contacts (less than the sum of the corresponding van der Waals radii) with six $[\text{BF}_4]^-$ anions (Table 1). The seventh anion resides on top of the $[\text{Emim}]^+$ ring, while the bottom position is occupied by another cation (Fig. 2).

This geometry reasonably well matches characteristics of the liquid $[\text{Emim}][\text{BF}_4]$ obtained from the ^1H , ^{19}F -HOESY NMR experiment,²¹ indicating strong contacts of all the cation protons with the anions (Table 1). It is also worth noting that the positions of the anions forming short contacts with the protons of the $[\text{Emim}]^+$ ring (Fig. S2, ESI[†]) closely resemble those found in crystals of $[\text{Emim}][\text{BF}_4]$ and revealed by the

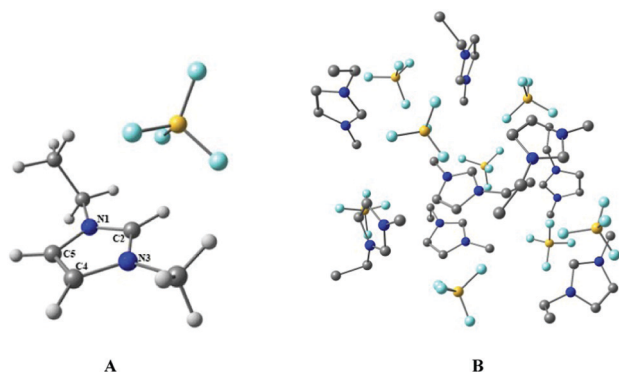


Fig. 1 The B97-3c optimized geometries of the $[\text{Emim}][\text{BF}_4]$ ion pair (A) and $([\text{Emim}][\text{BF}_4])_8$ cluster (B). Hydrogen atoms in the cluster are omitted for clarity. The atom numbering scheme is given for the imidazolium ring.

Table 1 Computed and experimental characteristics of H...F short contacts in [Emim][BF₄]

Protons participating in contacts with anions. See Fig. 1(A) for atom numbering	H...F distances (in Å) computed for the cluster shown in Fig. 1(B). The sum of van der Waals radii ≈ 2.6 Å	Relative cross relaxation rates between the protons and the anions in neat [Emim][BF ₄]. ²¹ The strongest interaction has been used for normalization
(C2)H	2.15	1
(C4)H	2.17	0.89
(C5)H	2.16	0.89
(N1)CH ₂	2.70	0.89
(CH ₂)CH ₃	2.48	0.75
(N3)CH ₃	2.33–2.45	0.89

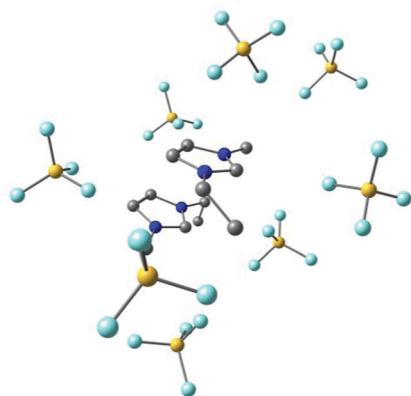


Fig. 2 The closest surrounding of the solvated [Emim]⁺ cation in the B97-3c optimized cluster ([Emim][BF₄])₈ shown in Fig. 1 (B). Hydrogen atoms are omitted for clarity.

analysis of the corresponding data-files from the Cambridge Structural Database.²²

3.2. IR spectra of ([Emim][BF₄])_n clusters, isolated [Emim]⁺ and [BF₄]⁻ ions, and their various associations

B97-3c computations of vibrational frequencies of the isolated ionic constituents of [Emim][BF₄] are in reasonably good agreement with the corresponding gas-phase experiment,⁴ providing practically the same quality of the spectra simulations as more time-demanding B3LYP/6-31+G(d,p) calculations (Table S1, ESI[†]). This suggests that B97-3c represents an adequate level of DFT approximation for simulation of the IR spectra of the IL under study.

Indeed, the IR spectrum simulated for cluster ([Emim][BF₄])₈ (Fig. 3b) quite well matches the corresponding experimental spectrum of the bulk [Emim][BF₄] liquid in the lower-frequency part (500–900 cm⁻¹) of the fingerprint region. Absorption saturation by the intense broad bands of stretching vibrations of the [BF₄]⁻ anion, $\nu_{\text{str}}(\text{BF}_4)$, in the bulk IR spectrum, prevents the simulation *vs.* experiment comparison of the IR intensities in the region ~ 1000 – 1100 cm⁻¹. Nevertheless, the positions of $\nu_{\text{str}}(\text{BF}_4)$ bands, known from attenuated total reflectance IR spectra^{23,24} of liquid [Emim][BF₄], are reproduced by our simulations for cluster

([Emim][BF₄])₈ reasonably well, in contrast to the computations of ion pair [Emim][BF₄] (Table 2). Much better quality of the spectra simulated for the cluster ([Emim][BF₄])₈ than for ion pair [Emim][BF₄] is also clearly seen from visual comparison of Fig. 3A and B.

It should be noted that the accurate comparison of our harmonic computations with the experiment is hampered by contamination of the region $> \sim 1100$ cm⁻¹ by combination bands and overtones.²⁵ These manifestations of anharmonism are most pronounced in the region of CH stretching vibrations, $\nu_{\text{str}}(\text{CH})$, critical for assessing hydrogen bonds (HBs) in the IL, which have become a topic of vigorous discussion (*e.g.* ref. 26–28). Deuteration of [Emim]⁺ at the C2 position allows the isolation of the band of $\nu_{\text{str}}(\text{C2D})$ from the Fermi resonance and other strong anharmonic effects, and its use as a convenient IR spectroscopic marker of HBs and other intermolecular interactions functioning in bulk IL and various gas-phase associations of the [Emim-d]⁺ cation.^{4,25} Our computations of the isolated cation perfectly reproduce the corresponding experimental value of $\nu_{\text{str}}(\text{C2D})$, while a small red shift of this band in the experimental IR spectrum of bulk liquid [Emim-d][BF₄]²⁰ relative to the gas-phase spectrum⁴ of [Emim-d]⁺ is qualitatively reproduced by the calculations of cluster ([Emim-d][BF₄])₈ (Table 3). The qualitatively incorrect blue shift of $\nu_{\text{str}}(\text{C2D})$ in the simulated spectra of the ([Emim-d][BF₄])_n species ($n = 4$ – 7) relative to the spectrum of [Emim-d]⁺ (Table 3) indicates that these models of bulk IL are oversimplified.

The above comparative analysis of $\nu_{\text{str}}(\text{C2D})$, as well as the fingerprint region (Fig. 3) in the spectrum simulated for an isolated ion pair, *i.e.* the simplest model of IL broadly used for interpretation of bulk IR spectra, and the spectrum computed for the ion pair solvated by the first solvation shell of other ion pairs, clearly demonstrates much better quality of the latter. This theoretical spectrum of the cluster ([Emim][BF₄])₈ matches the bulk IR experiment at least no worse than the simulated spectra of isolated [Emim]⁺, [BF₄]⁻, [Emim-d][BF₄]₂⁻ and [Emim-d]₂[BF₄]⁺ species match the corresponding gas-phase experiment⁴ (Tables S1–S3 (ESI[†]), respectively). This strongly suggests that, similar to the case of molecular liquids/solutions,^{8–10} the IR spectrum of the bulk IL is determined mainly by interaction of a minimal neutral entity, an ion pair, with its immediate surroundings, while the role of farther ions is minor, in spite of long-range Coulomb forces acting in such a medium.

3.3. Hydrogen bonding in bulk [Emim][BF₄] IL, and the gas-phase associations [Emim]₂[BF₄]⁺ and [Emim][BF₄]₂⁻

It is commonly accepted that intensification and red shift of the IR band of stretching vibrations of XH groups, $\nu_{\text{str}}(\text{XH})$, are the hallmarks of a HB involving XH as a donor. Quite modest red shift of $\nu_{\text{str}}(\text{C2D})$ in the spectrum of the bulk IL relative to the case of isolated [Emim]⁺, as well as a similarly small red shift reported for the gas-phase cationic cluster [Emim-d]₂[BF₄]⁺ (Table 3), were interpreted⁴ as an indication of very weak or even absent H-bonding in both cases. Nonetheless, as discussed in ref. 29, stretching frequencies of the CH groups

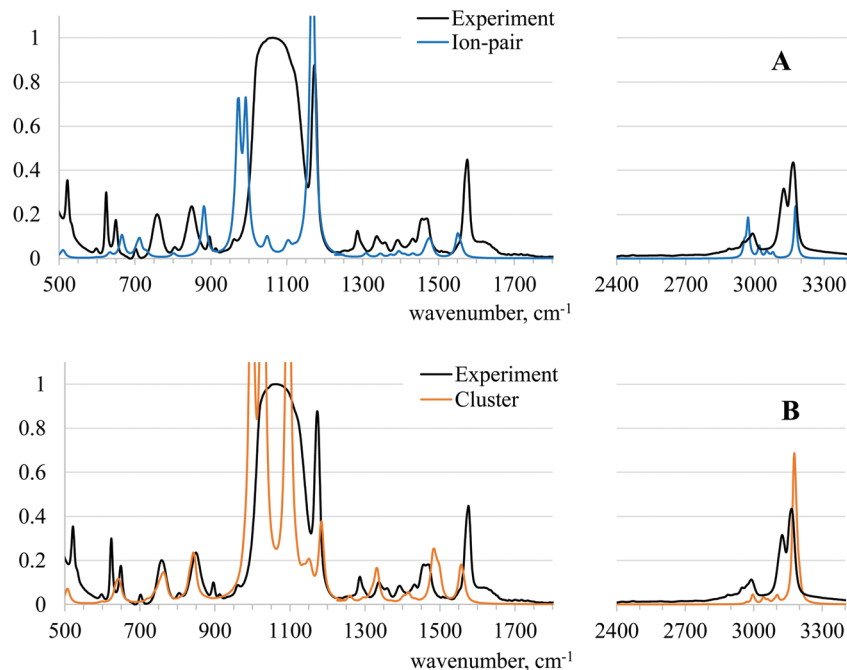


Fig. 3 Comparison of the experimental IR spectrum of liquid $[\text{Emim}][\text{BF}_4]^{20}$ with B97-3c simulated IR spectra of ion pair $[\text{Emim}][\text{BF}_4]$ (A), and of cluster $([\text{Emim}][\text{BF}_4])_8$ (B). The spectra are normalized so that the maximum experimental intensity is equal to unity, and the calculated and experimental intensities of the bands around 850 cm^{-1} coincide with each other.

Table 2 Experimental frequencies (cm^{-1}) of stretching vibrations of the $[\text{BF}_4]^-$ anion in bulk liquid $[\text{Emim}][\text{BF}_4]$,^{23,24} and frequencies computed for different models

Bulk IL (experiment)	1016	$\sim 1025/1033$	1046
Ion pair $[\text{Emim}][\text{BF}_4]$	972	992	1167
$([\text{Emim}][\text{BF}_4])_8$	997	1027	1097

Table 3 Experimental frequencies (in cm^{-1} , bold) of stretching vibrations $\nu_{\text{str}}(\text{C2D})$ of $[\text{Emim-d}]^+$ in gas (isolated cation and $[\text{Emim-d}][\text{BF}_4]_2^-$ anion),⁴ and in bulk liquid $[\text{Emim-d}][\text{BF}_4]^{20}$ and frequencies computed for various models scaled with 0.979 (the computed IR intensities in km mol^{-1} are given in parentheses)

$[\text{Emim-d}]^+$ (gas-phase experiment)	2362
$[\text{Emim-d}]^+$	2362 (9.3)
$[\text{Emim-d}][\text{BF}_4]_2^-$ (gas-phase experiment)	~ 2310
$[\text{Emim-d}][\text{BF}_4]_2^-$	2299 (143)
$[\text{Emim-d}]_2[\text{BF}_4]^+$ (gas-phase experiment)	~ 2350
$[\text{Emim-d}]_2[\text{BF}_4]^+$	2343 (244)
Bulk IL (experiment)	2358
$([\text{Emim-d}][\text{BF}_4])_4$	2389 (13.8)
$([\text{Emim-d}][\text{BF}_4])_5$	2379 (14.8)
$([\text{Emim-d}][\text{BF}_4])_6$	2368 (39.1)
$([\text{Emim-d}][\text{BF}_4])_7$	2375 (22.3)
$([\text{Emim-d}][\text{BF}_4])_8$	2361 (40.6)

of the imidazolium ring are influenced not only by red-shifting HBs but also by other secondary interactions, which may cause a blue shift. *E.g.*, it was demonstrated that the effects of $\text{CH}\cdots[\text{PF}_6]^-$ ²⁹ and $\text{CH}\cdots[\text{OAc}]^-$ ³⁰ HBs were overcompensated by multiple secondary interactions present in crystals, which

resulted in the net blue shift. Similar effects probably explain the blue shift of $\nu_{\text{str}}(\text{C2D})$ in the IR spectra of solid $[\text{Emim-d}][\text{Tf}_2\text{N}]$ and $[\text{Emim-d}]\text{Br}$ relative to the spectra of the melts.²⁸ Furthermore, even in the case of H-bonded pairs forming a “classical” two-center HB isolated in an innocent solvent or gas, the shift can be zero or even negative.³¹

In contrast, strengthening of the $\nu_{\text{str}}(\text{XH})$ IR band is one of the well-accepted criteria of HB formation.³² There exists a correlational equation³¹ linking HB enthalpy, $-\Delta H_{\text{HB}}$, and intensity of $\nu_{\text{str}}(\text{XH})$:

$$-\Delta H_{\text{HB}} [\text{kcal mol}^{-1}] = 0.29 \Delta I^{1/2} [\text{km mol}^{-1}] \quad (1)$$

here, $\Delta I^{1/2} = I^{1/2} - I_0^{1/2}$, where I is the IR intensity for the localized, uncoupled stretching vibration $\nu_{\text{str}}(\text{XH})$ of the X-H group participating in the HB as compared to the non-interacting group (I_0). Equation (1) is applicable to 1:1 H-bonded complexes, in particular formed by CH moieties,³¹ in which the $-\Delta H_{\text{HB}}$ values are lower than 15 kcal mol^{-1} .³³ Its applicability to $\text{CH}\cdots[\text{PF}_6]^-$ ²⁹ and $\text{CH}\cdots[\text{OAc}]^-$ ³⁰ HBs in ILs has been demonstrated on a limited number of examples.

To apply eqn (1) to our systems, the IR intensities have been calculated for isotope-isolated vibrations of the various associations of $[\text{Emim}]^+$ with $[\text{BF}_4]^-$ species (I) and the bare $[\text{Emim}]^+$ cation (I_0). For example, in the case of the $\text{C2H}\cdots[\text{BF}_4]^-$ HB all hydrogen atoms except for the (C2)H atom of the imidazolium ring were substituted by deuterium atoms. Such an approach results in $\nu_{\text{str}}(\text{CH})$ and the $-\Delta H_{\text{HB}}$ values collected in Table 4. Inspection of Table 4 clearly demonstrates all signatures of HBs for $[\text{Emim}][\text{BF}_4]_2^-$ and $[\text{Emim}]_2[\text{BF}_4]^+$ species: (i) red shift and (ii) intensification of $\nu_{\text{str}}(\text{C2H})$ and $\nu_{\text{str}}(\text{C4H})$, (iii) lengthening

Table 4 Geometric and spectroscopic parameters computed for [Emim]⁺ and its various associations. Frequencies (in cm⁻¹) of isotopically isolated stretching vibrations $\nu_{\text{str}}(\text{C2H})$, and the IR intensities in km mol⁻¹ (in parentheses); interatomic distances $r(\text{C2H})$ and $r(\text{H}\cdots\text{F})$, in Å; enthalpy of HB $\text{CH}\cdots[\text{BF}_4]^-$, $-\Delta H_{\text{HB}}$ (kcal mol⁻¹) according to eqn (1). The same parameters for C4H and C5H are given in italics

	$\nu_{\text{str}}(\text{C2H})^a$	$r(\text{C2H})$	$r(\text{H}\cdots\text{F})$. The sum of van der Waals radii ≈ 2.6 Å.		$-\Delta H_{\text{HB}}$
[Emim] ⁺	3174 (17)	1.074			
	<i>3176 (9)^b</i>	<i>1.074^b</i>			
	<i>3177 (9)^c</i>	<i>1.074^c</i>			
[Emim][BF ₄] ₂ ⁻	3075 (306)	1.080	1.961		3.9
	<i>3180 (239)^b</i>	<i>1.078^b</i>	<i>2.039^b</i>		<i>3.6^b</i>
[Emim] ₂ [BF ₄] ⁺	3143 (283)	1.076	2.111		3.7
([Emim] ₂ [BF ₄]) ₈	3175 (88)	1.072	2.150		1.5
	<i>3178 (52)^c</i>	<i>1.073^c</i>	<i>2.159^c</i>		<i>1.2^c</i>

^a Scaled with 0.979. ^b Computed for C4H. ^c Computed for C5H.

of the C2H and C4H bonds, and (iv) quite short H \cdots F contacts. $-\Delta H_{\text{HB}}$ values, estimated for these ions with the use of Eqn. (1), vary between 3.6 and 3.9 kcal mol⁻¹. In the case of cluster ([Emim][BF₄])₈ the signatures (i) and (iii) are absent. Nevertheless, short H \cdots F contacts, and *ca.* 5-fold increase of the IR intensity of $\nu_{\text{str}}(\text{C2H})$ and $\nu_{\text{str}}(\text{C5H})$ for ([Emim][BF₄])₈ relative to [Emim]⁺ suggests that C2H and C5H moieties of the imidazolium ring of ([Emim][BF₄])₈ still form HBs, though less pronounced than in the case of [Emim][BF₄]₂⁻ and [Emim]₂[BF₄]⁺ species. The use of Eqn. (1) produces estimates of $-\Delta H_{\text{HB}}$, which amount to *ca.* 1.5 kcal mol⁻¹ for C2H and *ca.* 1.2 kcal mol⁻¹ for C5H. Thus, CH moieties of the imidazolium ring form HBs of moderate strength in all the studied species, and the almost negligible red shift of $\nu_{\text{str}}(\text{C2D})$ relative to isolated [Emim]⁺ does not indicate negligible H-bonding in the ([Emim][BF₄])₈ cluster. The good match of the spectra simulated for this cluster to the experimental spectra of bulk IL (Section 3.2) strongly suggests that the above statement is also applicable to the bulk IL.

The estimates of $-\Delta H_{\text{HB}}$ for $\text{CH}\cdots[\text{BF}_4]^-$ HBs in the cluster model of liquid [Emim][BF₄] (Table 4) are of the same order of magnitude as the analogous estimate of the enthalpy of $\text{C2H}\cdots[\text{PF}_6]^-$ HB (2.1 kcal mol⁻¹)²⁹ obtained for crystals of 1-(2'-hydroxyethyl)-3-methylimidazolium hexafluorophosphate ([C₂OHmim][PF₆]). They are expectedly much smaller than the enthalpies of HBs formed by C2H and C5H moieties of the [C₂OHmim]⁺ cation with the much more HB-basic acetate anion [OAc]⁻ (4.9 and 5.4 kcal mol⁻¹, respectively) in crystals of [C₂OHmim][OAc].³⁰ Nevertheless, both [Emim][BF₄] and [C₂OHmim][OAc] bulk ILs have one common feature, namely, a rather moderate difference between the enthalpies of HBs formed by the C2H and C5H moieties of the imidazolium ring. This counterintuitive behavior of the C2H and C4H/C5H sites with the different acidity persists also in the case of the gas phase: the enthalpies of HBs $\text{C2H}\cdots[\text{BF}_4]^-$ and $\text{C4H}\cdots[\text{BF}_4]^-$ in isolated anion [Emim][BF₄]₂⁻ differ by less than 10% (Table 4). Another common specific of the above “non-conventional” charge-assisted HBs formed by CH moieties of the imidazolium ring is their significant strengthening in the gas phase relative to the bulk IL: *cf.* 3.9 or 3.7 kcal mol⁻¹ in isolated [Emim][BF₄]₂⁻

or [Emim]₂[BF₄]⁺ ions, respectively, *vs.* 1.5 kcal mol⁻¹ in ([Emim][BF₄])₈; and 10.4 kcal mol⁻¹ in the isolated [C₂OHmim][OAc] ion pair *vs.* 4.9 kcal mol⁻¹ in the corresponding crystal.³⁰

4. Conclusions

In this work, we applied an explicit solvation protocol for the quantum chemical simulation of the structure and IR spectra of bulk ILs [Emim][BF₄] and [Emim-d][BF₄]. We have shown that the solvation strongly modifies the frequencies and IR intensities of both cationic and anionic components of the ILs. The main features of the bulk spectrum are reproduced by the spectrum simulated for cluster ([Emim][BF₄])₈, representing an ion pair solvated by the first solvation shell comprising seven cations and seven anions. This strongly suggests that, similar to the case of molecular liquids/solutions, the impact of the remaining part of the surrounding medium on the IR spectrum of the solvated species is rather moderate. In other words, the influence of the electric field of the ions behind the first solvation shell of a solute on its dipole moment derivatives and force constants is quite moderate. This knowledge not only improves our understanding of solute-solvent interactions, but also allows minimization of the computational costs of quantum chemical simulations of the IR spectra of bulk ILs.

Good match of the simulated and experimental spectra suggests a close structural correspondence of the actual IL and model cluster ([Emim][BF₄])₈. Geometries of the latter cluster and, most probably, of actual IL closely resemble the solid-state structure of [Emim][BF₄] and are characterized by short contacts of all CH moieties of the imidazolium ring with [BF₄]⁻ anions. Both structural and spectroscopic analyses allow the contacts to be interpreted as H-bonds of approximately equal strength. The combined action of the HBs and other condensed-state forces induces quite moderate red shifts of the IR bands of stretching vibrations of the CH moieties, and *ca.* 5-fold increase of their intensity relative to the case of an isolated [Emim]⁺ cation. Enthalpies of the liquid-state $\text{CH}\cdots[\text{BF}_4]^-$ HBs, estimated on the basis of quantitative characteristics of this intensification with the use of empirical correlations, amount to 1.2–1.5 kcal mol⁻¹, while the enthalpies are more than doubled in the negatively and positively charged gas-phase associations of ionic components of the IL. This disparity, already marked in the case of another IL, [C₂OHmim][OAc],³⁰ suggests that an analysis of the role of H-bonding in ILs based solely on “gas-phase” computations can lead to the misinterpretation of the data. Reliable simulations of both the gas-phase, and the liquid-state IR spectra within the framework of our cluster approach deliver confidence in reliability of modeling of other properties of the actual systems in both states. The quantitative analysis described herein should facilitate further studies on the role of hydrogen bonding in ILs and ultimately it could aid the rational design of ILs with specific physical and chemical properties.

Conflicts of interest

There are no conflicts of interest to declare.

Acknowledgements

The authors are grateful to Prof. S. Grimme for permission to use program QCG¹¹ and computational facilities of Mulliken Center for Theoretical Chemistry (Institut für Physikalische und Theoretische Chemie der Universität Bonn). Useful advice from Prof. P. M. Tolstoy, and Dr E. Y. Tupikina is gratefully acknowledged (SAK).

References

- 1 F. Philippi and T. Welton, Targeted modifications of ionic liquids – from understanding to design, *Phys. Chem. Chem. Phys.*, 2021, **23**, 6993–7021.
- 2 V. H. Paschoal, L. F. O. Faria and M. C. C. Ribeiro, Vibrational Spectroscopy of Ionic Liquids, *Chem. Rev.*, 2017, **117**, 7053–7112.
- 3 S. A. Katsyuba, E. E. Zvereva and T. I. Burganov, Is there a simple way to reliable simulations of infrared spectra of organic compounds?, *J. Phys. Chem. A*, 2013, **117**, 6664–6670.
- 4 C. J. Johnson, J. A. Fournier, C. T. Wolke and M. A. Johnson, Ionic liquids from the bottom up: Local assembly motifs in [Emim][BF₄] through cryogenic ion spectroscopy, *J. Chem. Phys.*, 2013, **139**, 224305.
- 5 M. Praprotnik, D. Janezic and J. Mavri, Temperature Dependence of Water Vibrational Spectrum: A Molecular Dynamics Simulation Study, *J. Phys. Chem. A*, 2004, **108**, 11056–11062.
- 6 J. Stare, J. Mavri, J. Grdadolnik, J. Zidar, Z. B. Maksic and R. Vianello, Hydrogen Bond Dynamics of Histamine Monocation in Aqueous Solution: Car-Parrinello Molecular Dynamics and Vibrational Spectroscopy Study, *J. Phys. Chem. B*, 2011, **115**, 5999–6010.
- 7 M. Thomas, M. Brehm, R. Fligg, P. Vöhringer and B. Kirchner, Computing vibrational spectra from *ab initio* molecular dynamics, *Phys. Chem. Chem. Phys.*, 2013, **15**, 6608–6622.
- 8 S. A. Katsyuba, S. Spicher, T. P. Gerasimova and S. Grimme, Revisiting Conformations of Methyl Lactate in Water and Methanol, *J. Chem. Phys.*, 2021, **155**, 024507.
- 9 S. A. Katsyuba, S. Spicher, T. P. Gerasimova and S. Grimme, Fast and Accurate Quantum Chemical Modeling of Infrared Spectra of Condensed-Phase Systems, *J. Phys. Chem. B*, 2020, **124**, 6664–6670.
- 10 S. A. Katsyuba, T. P. Gerasimova, S. Spicher, F. Bohle and S. Grimme, Computer-aided Simulation of Infrared Spectra of Ethanol Conformations in Gas, Liquid and in CCl₄ Solution, *J. Comput. Chem.*, 2022, **43**, 279–288.
- 11 S. Spicher and S. Grimme, to be submitted. Please contact grimme@thch.uni-bonn.de for the QCG program.
- 12 S. Grimme, C. Bannwarth, E. Caldeweyher, J. Pisarek and A. Hansen, A general intermolecular force field based on tight-binding quantum chemical calculations, *J. Chem. Phys.*, 2017, **147**, 161708.
- 13 C. Bannwarth, S. Ehlert and S. Grimme, GFN_{2-x}TB – An Accurate and Broadly Parametrized Self-Consistent Tight-Binding Quantum Chemical Method with Multipole Electrostatics and Density-Dependent Dispersion Contributions, *J. Chem. Theory Comput.*, 2019, **15**, 1652–1671.
- 14 J. G. Brandenburg, C. Bannwarth, A. Hansen and S. Grimme, B97-3c: A revised low-cost variant of the B97-D density functional method, *J. Chem. Phys.*, 2018, **148**, 064104.
- 15 S. A. Katsyuba, E. E. Zvereva and S. Grimme, Fast Quantum Chemical Simulations of Infrared Spectra of Organic Compounds with the B97-3c Composite Method, *J. Phys. Chem. A*, 2019, **123**, 3802–3808.
- 16 E. E. Zvereva, A. R. Shagidullin and S. A. Katsyuba, *Ab Initio* and DFT Predictions of Infrared Intensities and Raman Activities, *J. Phys. Chem. A*, 2011, **115**, 63–69.
- 17 F. Furche, R. Ahlrichs, C. Hättig, W. Klopper, M. Sierka and F. Weigend, TURBOMOLE V7.5.1 2021, a development of University of Karlsruhe and Forschungszentrum Karlsruhe GmbH, 1989–2007, TURBOMOLE GmbH since 2007; available from <http://www.turbomole.com>.
- 18 Y. Umabayashi, T. Fujimori, T. Sukizaki, M. Asada, K. Fujii, R. Kanzaki and S. Ishiguro, Evidence of Conformational Equilibrium of 1-Ethyl-3-methylimidazolium in its Ionic Liquid Salts: Raman Spectroscopic Study and Quantum Chemical Calculations, *J. Phys. Chem. A*, 2005, **109**, 8976–8982.
- 19 N. E. Heimer, R. E. Del Sesto, Z. Z. Meng, J. S. Wilkes and W. R. Carper, Vibrational Spectra of Imidazolium Tetrafluoroborate Ionic Liquids, *J. Mol. Liq.*, 2006, **124**, 84–95.
- 20 S. A. Katsyuba, E. E. Zvereva, A. Vidiš and P. J. Dyson, Application of Density Functional Theory and Vibrational Spectroscopy toward the Rational Design of Ionic Liquids, *J. Phys. Chem. A*, 2007, **111**, 352–370.
- 21 Y. Lingscheid, S. Arenz and R. Giernoth, Heteronuclear NOE spectroscopy of Ionic Liquids, *ChemPhysChem*, 2012, **13**, 261–266.
- 22 E. E. Zvereva, S. A. Katsyuba and P. J. Dyson, A Simple Physical Model for The Simultaneous Rationalisation of Melting Points and Heat Capacities of Ionic Liquids, *Phys. Chem. Chem. Phys.*, 2010, **12**, 13780–13787.
- 23 T. Yamada and M. Mizuno, Infrared Spectroscopy in the Middle Frequency Range for Various Imidazolium Ionic Liquids – Common Spectroscopic Characteristics of Vibrational Modes with In-Plane ¹³C(2)–H and ¹³C(4,5)–H Bending Motions and Peak Splitting Behavior Due to Local Symmetry Breaking of Vibrational Modes of the Tetrafluoroborate Anion, *ACS Omega*, 2021, **6**, 1709–1717.
- 24 A. Shalygin, N. S. Nesterov, S. A. Prikhod'ko, N. A. Adonin, O. N. Martyanov and S. G. Kazarian, Interactions of CO₂ with the homologous series of C_nMIMBF₄ ionic liquids studied in situ ATR-FTIR spectroscopy: spectral characteristics, thermodynamic parameters and their correlation, *J. Mol. Liq.*, 2020, **315**, 113694.
- 25 J. A. Fournier, C. T. Wolke, C. J. Johnson, A. McCoy and M. A. Johnson, Comparison of the local binding motifs in the imidazolium-based ionic liquids [EMIM][BF₄] and [EMMIM][BF₄] through cryogenic ion vibrational predissociation spectroscopy: Unraveling the roles of anharmonicity

- and intermolecular interactions, *J. Chem. Phys.*, 2015, **142**, 064306.
- 26 J.-C. Lassegues, J. Grondin, D. Cavagnat and P. Johansson, New Interpretation of the CH Stretching Vibrations in Imidazolium-Based Ionic Liquids, *J. Phys. Chem. A*, 2009, **113**, 6419–6421.
- 27 A. Wulf, K. Fumino and R. Ludwig, Comment on “New Interpretation of the CH Stretching Vibrations in Imidazolium-Based Ionic Liquids”, *J. Phys. Chem. A*, 2010, **114**, 685–686.
- 28 J. Grondin, J.-C. Lassegues, D. Cavagnat, T. Buffeteau, P. Johansson and R. Holomb, Revisited Vibrational Assignments of Imidazolium-Based Ionic Liquids, *J. Raman Spectrosc.*, 2011, **42**, 733–743.
- 29 S. A. Katsyuba, M. V. Vener, E. E. Zvereva, Z. Fei, R. Scopelliti, G. Laurency, N. Yan, E. Paunescu and P. J. Dyson, How Strong Is Hydrogen Bonding in Ionic Liquids? Combined X-ray Crystallographic, Infrared/Raman Spectroscopic, and Density Functional Theory Study, *J. Phys. Chem. B*, 2013, **117**, 9094–9105.
- 30 S. A. Katsyuba, M. V. Vener, E. E. Zvereva, Z. Fei, R. Scopelliti, Y. G. Brandenburg, S. Siankevich and P. J. Dyson, Quantification of Conventional and Non-conventional Charge-Assisted Hydrogen Bonds in the Condensed and Gas Phases. *J. Phys. Chem. Lett.*, 2015, **6**, 4431–4436.
- 31 A. V. Iogansen, Direct Proportionality of the Hydrogen Bonding Energy and the Intensification of the Stretching $\nu(\text{XH})$ Vibration in Infrared Spectra, *Spectrochim. Acta, Part A*, 1999, **55**, 1585–1612.
- 32 E. Arunan, G. R. Desiraju, R. A. Klein, J. Sadlej, S. Scheiner, I. Alkorta, D. C. Clary, R. H. Crabtree, J. J. Dannenberg, P. Hobza, H. G. Kjaergaard, A. C. Legon, B. Menucci and D. J. Nesbitt, Definition of the Hydrogen Bond (IUPAC Recommendations 2011), *Pure Appl. Chem.*, 2011, **83**, 1637–1641.
- 33 E. Y. Tupikina, P. M. Tolstoy, A. I. Titova, M. A. Kostin and G. S. Denisov, Estimations of $\text{FH}\cdots\text{X}$ hydrogen bond energies from IR intensities: Iogansens’s rule revisited, *J. Comput. Chem.*, 2021, **42**, 564–571.